ADVANCES IN ATMOSPHERIC SCIENCES, VOL. 27, NO. 4, 2010, 795–806

Convective Asymmetries Associated with Tropical Cyclone Landfall: β-Plane Simulations

HUANG Wei* (黄 伟) and LIANG Xudong (梁旭东)

Shanghai Typhoon Institute, China Meteorological Administration, 166 *Puxi Road, Shanghai* 200030

(Received 13 April 2009; revised 1 September 2009)

ABSTRACT

The physical processes associated with changes in the convective structure of an idealized tropical cyclone (TC) during landfall on a beta-plane were studied using the fifth-generation Pennsylvania State University–National Center for Atmospheric Research Mesoscale Model, version 3 (MM5). The simulation results suggested that the suppression of moisture supply and increased friction acted to enhance the convection from the left and front quadrants of the TC to the front and right of the TC during different periods of landfall. When surface moisture flux was turned off, convection in other parts of the quadrant was clearly suppressed and the total rainfall was reduced. When surface friction was increased, precipitation showed a marked increase after the TC made landfall.

Wetter air at low and intermediate levels, and drier air at high levels around the onshore side of the coastline led to a high value of convective available potential energy (CAPE). Consequently, convection was enhanced immediately downstream of this area when the surface moisture flux was cut off. When surface friction was increased, the physical process was similar prior to landfall. After landfall, increased convergence at the onshore side of the land resulted in enhanced convection in front of the TC.

Consistent with previous findings, our results suggest that during landfall the TC structure changes from one of thermodynamic symmetry to asymmetry due to differential moisture flux between the land and sea surface. The asymmetry of the thermodynamic structure, which can be explained by the distribution of CAPE, causes an asymmetric rainfall structure.

Key words: tropical cyclone, landfall, convective asymmetry

Citation: Huang, W., and X. D. Liang, 2010: Convective asymmetries associated with tropical cyclone landfall: β-plane simulations. *Adv. Atmos. Sci.*, **27**(4), 795–806, doi: 10.1007/s00376-009-9086-3.

1. Introduction

When a tropical cyclone (TC) moves close to land, the boundary-layer conditions change due to modification of the latent and sensible heat fluxes and increased roughness over land. These changes tend to produce highly asymmetric structures in a landfalling TC, which not only affect the intensity and track, but also the distribution of precipitation and wind gusts. Because most damage caused by TCs occurs in the coastal zone, understanding how the asymmetric structure arises during TC landfall and specifying the structure and organization of the storm is of great importance. Previous observational studies have provided detailed analyses of surface wind and rainfall characteristics at landfall for individual TCs (e.g. Miller, 1964; Powell, 1982, 1987; Powell and Houston, 1996, 1998; Blackwell, 2000; Chan et al., 2004; Schneider and Barnes, 2005); however, a lack of data has prevented scientists from gaining a thorough understanding of the underlying physical processes.

In idealized TC-landfall modeling studies, Tuleya and Kurihara (1978) and Tuleya et al. (1984) reported the development of considerable convective asymmetries due to asymmetric surface fluxes. Chan and Liang (2003; hereafter CL03) simulated TC landfall on an f-plane using the Pennsylvania State University-National Center for Atmospheric Research (PSU-NCAR) Mesoscale Model version 5 (MM5), investigating the effects of sensible heat flux, moisture flux, and increased roughness over land on an f-plane on distribution of convection. Their results suggested that moisture supply is the dominant factor in modifying the convective structure, whereas the sensible heat flux

*Corresponding author: HUANG Wei, huangw@mail.typhoon.gov.cn

has little effect. Prior to landfall, maximum precipitation was found in the front and left quadrants of the TC, but after landfall (when surface moisture flux was turned off and surface roughness increased) it occurred in the front and right quadrants. In their paper, a conceptual experiment, in which moisture supply only occurs over the ocean, showed that dry air over land was advected upward and around such that atmospheric stability was reduced at some locations. The results of more realistic numerical experiments have demonstrated that convective instability is indeed greatest immediately upstream of the maximum rainfall. In other words, a change in moisture supply affects the convection distribution during TC landfall via modification of the moist static stability of the atmosphere.

The simulation described in CL03 was performed on an f-plane. Because the β-effect contributes toward wind asymmetry and even convective asymmetry (e.g. Kwok and Chan, 2005), it is important to study the asymmetric structure of a TC during landfall on a β-plane to test the validity of the mechanism, proposed in CL03, in which modification of the moist static stability plays a key role on the distribution of convection of the TC.

The objective of the present study was to investigate convective asymmetries during the landfall of a TC on a β-plane, as a follow-up to the work of CL03. The remainder of the paper is organized as follows. The numerical experiments are described in section 2, and the effects of moisture supply and roughness over land are considered in section 3. In sections 4 and 5, we consider the processes which might explain the simulation results. And finally, section 6 summarizes the results and discusses the possible influence of the coastline on the distribution of convection.

2. Model and experiments

The numerical model used for this study was version three of the fifth-generation Pennsylvania State University–Mesoscale National Center for Atmospheric Research Model 5 (MM5; Dudhia, 1993; Grell et al., 1994). The model employed the Betts–Miller cumulus parameterization (Betts and Miller, 1993; Janjic, 1994), a simple ice scheme (Dudhia, 1989), and the high-resolution Blackadar planetary boundary layer (PBL) scheme (Blackadar, 1979; Zhang and Anthes, 1982). The horizontal resolution was 15 km and there were 301 grid points in the x and y directions, yielding an experimental domain of 4500 × 4500 km^2. Sixteen full σ-layers (1.0, 0.99, 0.97, 0.94, 0.90, 0.85, 0.79, 0.71, 0.61, 0.49, 0.37, 0.27, 0.18, 0.10, 0.04, and 0.00) were used in the vertical. This setup was the same as in CL03, thereby enabling a comparison of the results of the two studies.

The center latitude was set at 20°N and the Coriolis parameter varied as $f = f_0 + \beta \times y$, where $\beta = df/dy, f_0 = f(20°)$; in CL03, $f = f(20°)$. The initial fields of all experiments were obtained by integrating a pre-specified vortex for 36 hours in a quiescent atmospheric environment, as described in Chan et al. (2001) and CL03. As f was not constant in this study, the initial location of the TC was at the grid (142, 164) instead of (151, 151) as used in CL03. All integrations were carried out for 36 hours.

The control experiment was run with ocean planetary boundary layer (PBL) conditions over the entire domain, similar to the control run in CL03. To simulate the effect of land on the distribution of convection, three experiments were performed with different PBL parameters. Experiment 1 was similar to experiment 3 in CL03, where latent heat flux over land was turned off. The roughness length over land was set at 0.25 cm in experiment 2, the same as in experiment 4 in CL03. In experiment 3, moisture supply and roughness length were increased over land. In all experiments, land use at each grid point was set as "water body." In other words, the land in each experiment was not real land, but merely an area over which one parameter was changed. This approach enabled us to isolate the effect of surface moisture flux from land areas and the effect of friction on momentum transfer in the two experiments. Given that sensible heat flux showed a negligible effect on convection, we do not describe the experiment in which sensible heat flux was turned off over land.

As f was fixed in CL03, the coastline was moved to avoid asymmetries due to the steering current. In the present study, the TC was able to move northwestward in the β-plane without a steering current; therefore, the coastline was oriented approximately northeast–southwest (30° east of north) to ensure that the TC made landfall after around 27 hours of integration (see Fig. 1).

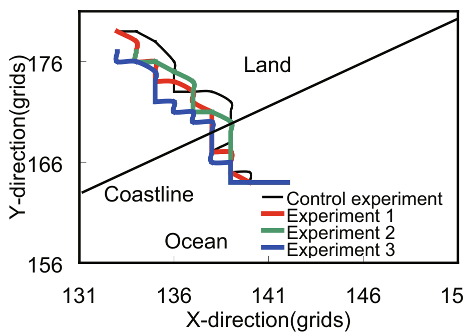

Fig. 1. Tracks of TC centers in the four experiments (over the period 36–72 hours, at 3-hour intervals).

3. Response to the PBL flux effect

3.1 *Track and intensity*

The position of the central lowest pressure was used to define the TC center. As expected, the TC in all experiments moved northwestward (e.g. Chan and Williams, 1987) (Fig. 1). Compared with the control experiment, the TCs in experiments 1–3 veered to the left, with the TC in experiment 3 having had the largest left-veering bias. This result shows that landfall may cause a TC to move to the left, which is consistent with the results of Szeto and Chan (2007), who also provided a physical explanation of this deflection. Accordingly, this issue is not further considered in the present paper.

The TC in the control experiment maintained an approximately constant intensity, but the minimum surface layer pressure (MSLP) was about 20 hPa higher than that in the control experiment of CL03 (Fig. 2). This finding is consistent with the results of Kwok and Chan (2005) and Peng et al. (1999), who reported that a TC on a β-plane intensifies at a slower rate than that on an f-plane. The evolution of TCs in the other three experiments showed three distinct stages: a fluctuating stage (as with the control experiment) before 15 hours, a gradually weakening stage from 16–25 hours, and a rapid weakening stage after 26 hours. The results were slightly different from those of Tuleya and Kurihara (1978) in that before landfall, the three TCs experienced a slight weakening, whereas the TC in the control experiment showed a slow deepening. Many studies have described a rapid weakening of TCs after landfall (Chen and Yau, 2003; Tuleya et al., 1984).

3.2 *Rainfall distribution*

Following CL03, temporal variations in precipitation were obtained by summing the hourly rainfall within each 15 km, 1° azimuth box (centered on the TC center) out to 300 km, although in the present study the 90° azimuth was set to be the right-hand side of the coastline instead of the north (Fig. 3). The azimuth of 180° represents the front side of the TC. As in CL03, the rainbands in the control experiment rotated cyclonically around the TC center (Fig. 3a), although the rainfall amount was less than that in CL03 due to decreased intensity. Because the asymmetric flow of the β-gyres acted to enhance the inward radial wind in the southeast part of the TC and the tangential wind in the northeastern part (Peng et al., 1999), the maximum rainfall of the TC was always located in the southeast to northeast quadrants. In other words, the highest rainfall tended to occur in the right quadrant of the TC, consistent with the results of Shapiro (1983).

In experiment 1, the latent heat flux (surface moisture flux) over land (i.e. the front side of the TC) was cut off. Compared with the control experiment, the maximum rainfall in this experiment was located mainly at the right-front side of the TC (Fig. 3b). Before 12 hours, no significant difference existed between experiment 1 and the control (Fig. 4a). From 13–22 hours, however, the most strongly enhanced rainfall occurred in the left-front and front quadrants, and rainfall was reduced in the rear-right and rear-left quadrants compared with the control experiment. After landfall, enhanced rainfall occurred in the right-front to right quadrants. Thus, the maximum rainfall rotated from the left-front (before landfall) to the right-front (after landfall) of the TC. In experiment 3 in CL03, maximum rainfall was generally found ahead of the TC and in the forward-left quadrant. Note that in the present study, when the TC approached land and finally made landfall, the band of maximum rainfall moved slowly and anti-cyclonically (Fig. 3b).

In experiment 2, the asymmetric structure of rainfall was similar to that in the control experiment before landfall (Fig. 3c); however, when the TC was about 100 km from the coast (11 hours), rainfall was enhanced in the rear and left to left-front sectors (Fig. 4b). When the TC was close to the coast and finally made landfall, the area of enhanced rainfall shifted to the left-front and gradually to the right-front (Figs. 3c and 4b); i.e. from the left to the right quadrant. Overall, the rainfall in experiment 2 showed less asymmetry in its distribution than that in experiment 1 due to the enhanced rainfall in the front sector and slight reduction in the rear sector. As with experiment 1, the difference between experiment 2 of the present study and experiment 4 of CL03 was that in CL03 the enhanced rainfall was to the left of the TC even after landfall, whereas the bulk of the area of enhanced rainfall in

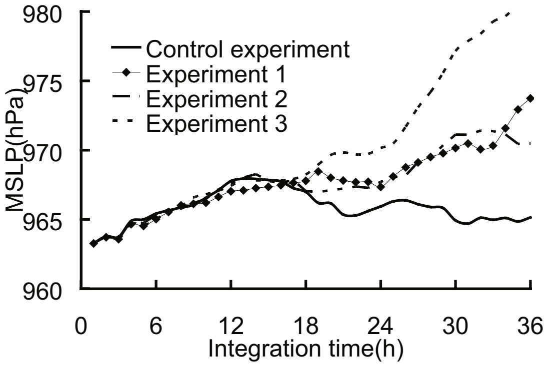

Fig. 2. Minimum sea-level pressure of the TC in each of the four experiments.

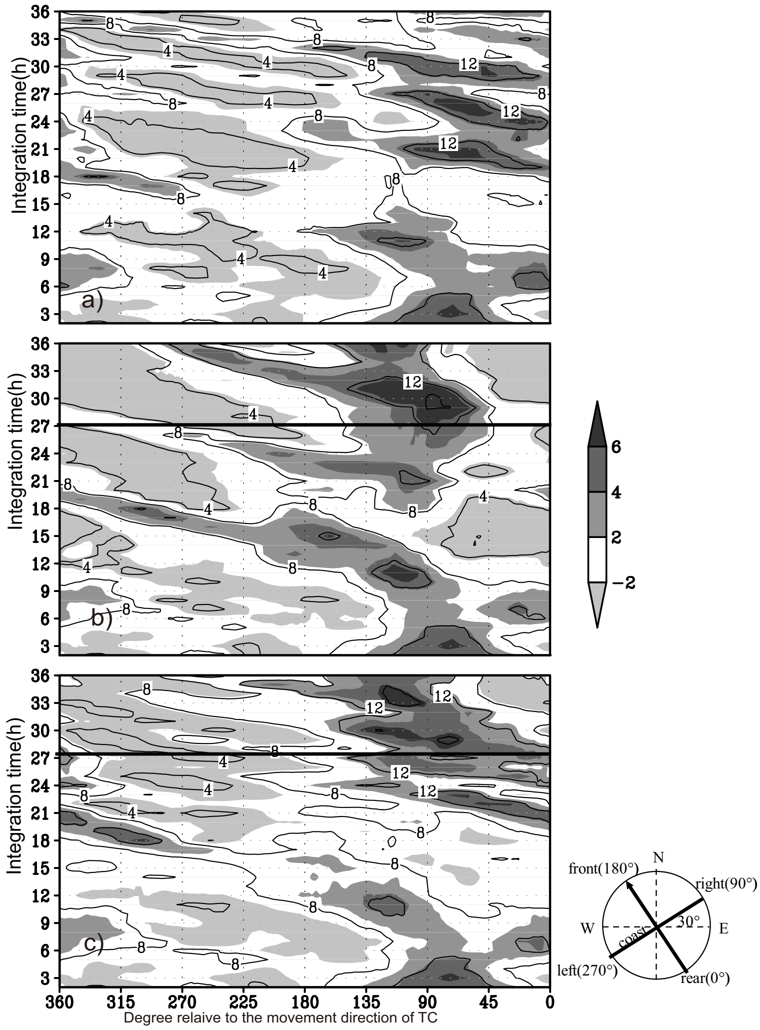

Fig. 3. Total hourly rainfall within 300 km at each azimuth from 1–36 hours after the vortex had been spun up for 36 hours for (a) the control run, (b) experiment 1, and (c) experiment 2. Shading indicates the asymmetric distribution of precipitation. The horizontal line at 27 hours in (b) and (c) indicates the time when the vortex center crossed the coast.

experiment 2 of the present study shifted to the right of the TC after landfall. After landfall, the maximum rainfall became more pronounced and moved from the right-rear quadrant to the right-front, suggesting that increased friction may play an important role in the development of an asymmetric TC structure after landfall.

The rainfall distribution in experiment 3 showed a pattern that combines the results of experiments 1 and 2 and that is similar to that in experiment 1 before landfall (data not shown). This finding indicates that moisture supply may play a more important role than roughness over land in determining the convection structure of a TC, especially before landfall. After landfall, moisture and roughness act together to influence the convection of the TC.

3.3 *Total rainfall*

The most significant difference between experiment 1 of the present study and that in CL03, in terms of total hourly rainfall within 300 km of the TC center, was that in the present study the rainfall was less than that in the control experiment (Fig. 5), indicating a possible reduction in precipitation with the suppression of moisture flux once the TC made landfall. The total rainfall in experiment 2 exceeded that in the control experiment, especially after landfall, when a rapid increase in rainfall occurred. These features are consistent with the average precipitation in the S1 and S2 experiments of Tuleya and Kurihara (1978). As might

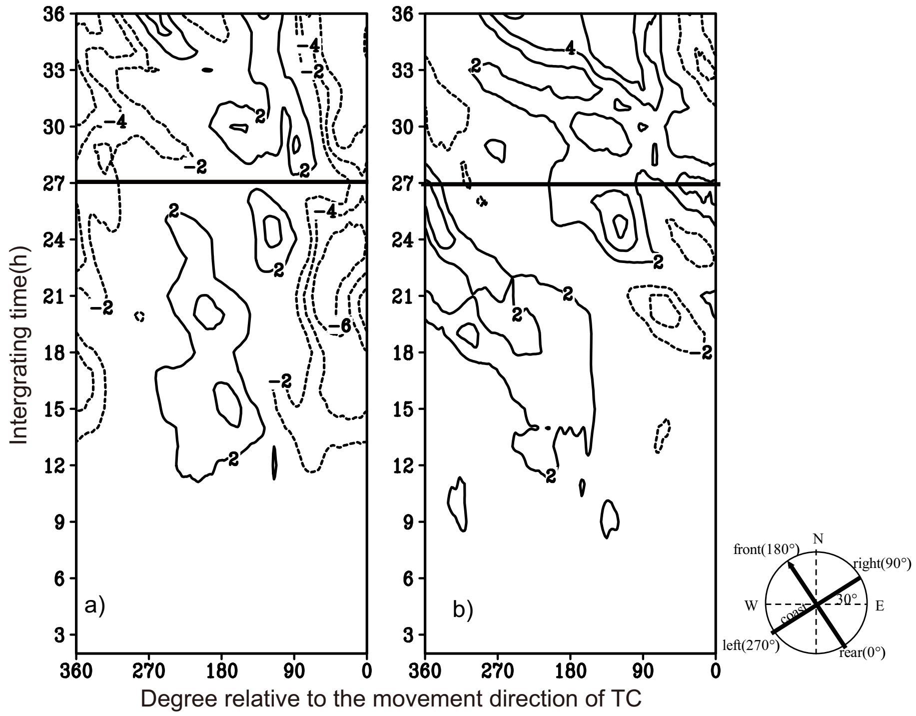

Fig. 4. Difference in rainfall compared with the control experiment: (a) experiment 1; (b): experiment 2 (units: cm). The horizontal line at 27 hours indicates the time when the vortex center crossed the coast.

be expected, the total rainfall in experiment 3 was less than that in experiment 2 and more than that in experiment 1, indicating that the reduction in moisture supply and increase in friction over land may play contrary roles in affecting precipitation during TC landfall.

4. Effect of moisture supply

CL03 suggested that cutting off the moisture flux from the land surface would decrease the amount of water vapor in the air; subsequently, the drier air may be advected into the TC center. However, the drier air may not result in reduced precipitation everywhere, as it may affect the instability of the air column as a consequence of horizontal and vertical advection. To determine if this type of physical process occurred in experiment 1, the potential pseudoequivalent temperature, θ_{se} (Bolton, 1980) was calculated. As the heaviest rainfall occurred within 100 km of the TC center, we considered the values of θ_{se} within 150 km. It is important to note that because the aim of the present study is to isolate the effect of landfall on distribution of convection, the results relative to those in the control experiment are generally of more importance than the results themselves.

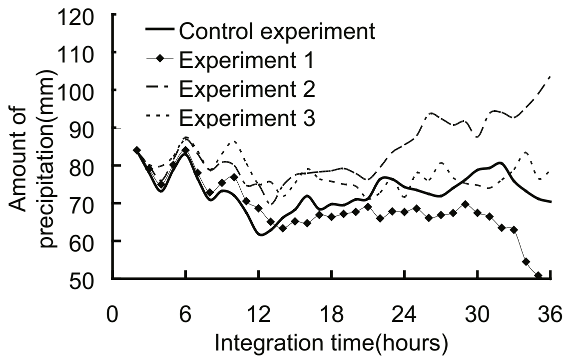

Fig. 5. Hourly total rainfall within 300 km of the TC center in the four experiments.

The average θ_{se} within 150 km of the TC center at each azimuth from 1–36 hours at σ-level 3 ($\sim$920 hPa) revealed that when the TC gradually approached the coast and finally made landfall, drier air occupied most of the area (Fig. 6a). This dominance of dry air resulted from two possible processes: (1) rotation of the TC causing the drier air to be advected cyclonically from front to left and then to the rear, and (2) the source of the drier air moving anti-cyclonically relative to the TC once the TC neared land. After landfall, the influence of the suppressed moisture supply expanded to the entire area except the right-rear quadrant. There existed a zone in which the air had a

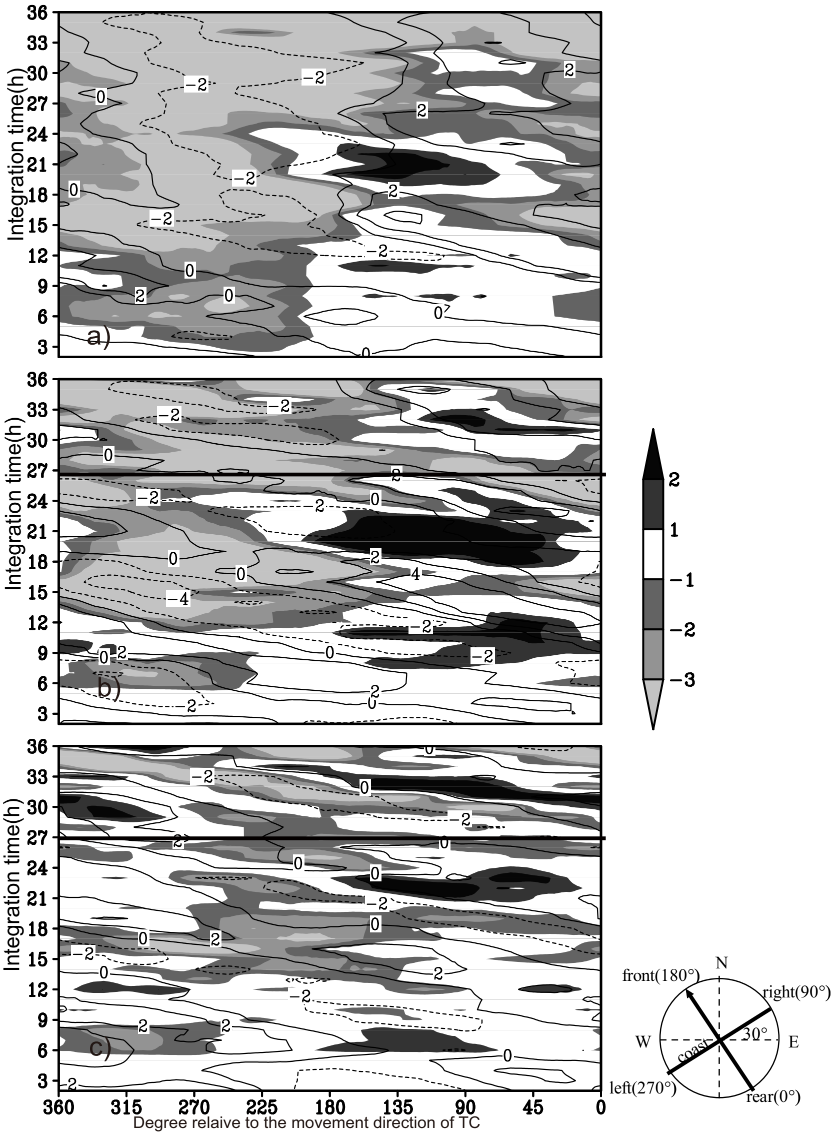

Fig. 6. Temporal evolution of θ_{se} at different vertical levels: (a) σ-level 3; (b) σ-level 5; (c) σ-level 7 in experiment 1 (contours: asymmetric distribution; shading: compared with the control run). The horizontal line at 27 hours indicates the time when the vortex center crossed the coast.

higher θ_{se} value than in the control experiment. Even after landfall, this area retained a higher θ_{se} value than in any other quadrant of the TC. At σ-level 5 ($\sim$850 hPa), the basic pattern of θ_{se} was similar to that at lower levels (Fig. 6b). Higher θ_{se} values were observed in similar quadrants to those at lower levels (around 90°); i.e. this area was located along the coastline, with winds blowing from the ocean. This was the last area occupied by relatively dry air from land, as the dry air rotated cyclonically.

At σ-level 7 ($\sim$750 hPa) , the θ_{se} value of the air around 90° dipped below the value in the control experiment (Fig. 6c). The air with lower θ_{se} values also influenced other areas via horizontal and vertical advection. In experiment 1, although most of the air had lower θ_{se} values at low levels (Figs. 6a–c), some air with high θ_{se} values was observed in a related stationary quadrant of the TC. When the TC approached land, this area with high θ_{se} values showed a slight clockwise shift. At the same time, the θ_{se} value of mid-level air in this place showed a slight decrease, which may lead to a marked increase in the instability of the air.

To further evaluate the convective potential of the atmosphere, the convective available potential energy (CAPE) was calculated. The formal definition of

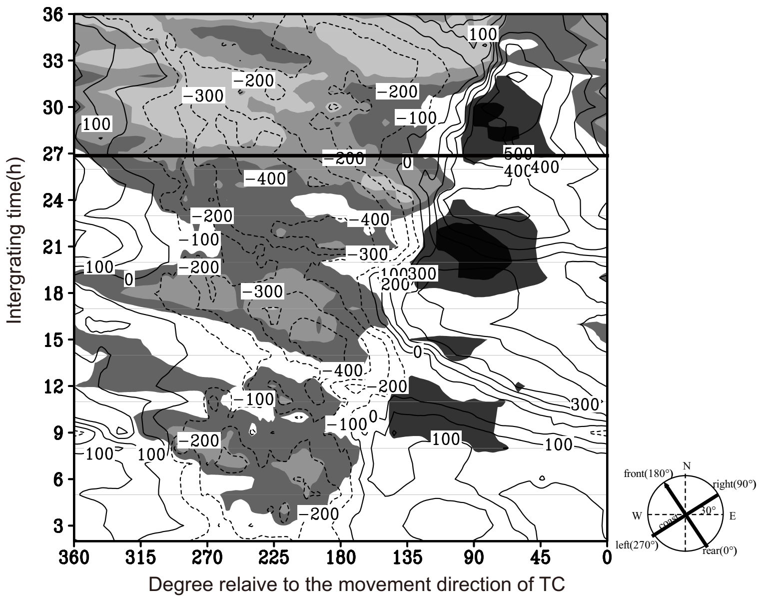

Fig. 7. Temporal evolution of CAPE in experiment 1 (contours: asymmetric distribution; shading: compared with the control run; units: J kg^{-1}). The horizontal line at 27 hours indicates the time when the vortex center crossed the coast.

CAPE is given by:

$$\mathrm{CAPE} = g\int_{Z_{\mathrm{lfc}}}^{Z_{\mathrm{el}}} \frac{T_{\mathrm{vp}} - T_{\mathrm{ve}}}{T_{\mathrm{ve}}} dz \,, \quad (1)$$

where T_{vp} is the virtual temperature of the air parcel, T_{ve} is the virtual temperature of the environment, Z_{el} is the height of the equilibrium level, Z_{lfc} is the level of free convection, and g is gravity. This definition of CAPE follows the method described by Doswell and Rasmussen (1994).

Consistent with the vertical distribution of θ_{se}, positive CAPE showed a stationary distribution around 90° (Fig. 7). Of note is the fact that positive CAPE was associated with positive θ_{se} values at intermediate levels (σ-level 5) and negative θ_{se} values at high levels (σ-level 7).

In examining the rainfall distribution in experiment 1, positive CAPE was associated with positive rainfall downstream of the TC. It is important to explain this relationship. Because the rainfall maxima before and after landfall occurred at distinct sites, it was possible to separate periods prior to landfall (11–23 hours) and after landfall (24–36 hours). Figure 8 shows the distribution of the anomalies, which means the difference from the control experiment in θ_{se}, vertical motion, CAPE, and rainfall around the TC. At this period, from 45° to 180°, θ_{se} showed a positive anomaly at low levels and a small negative anomaly at intermediate levels. Accordingly, the CAPE anomaly

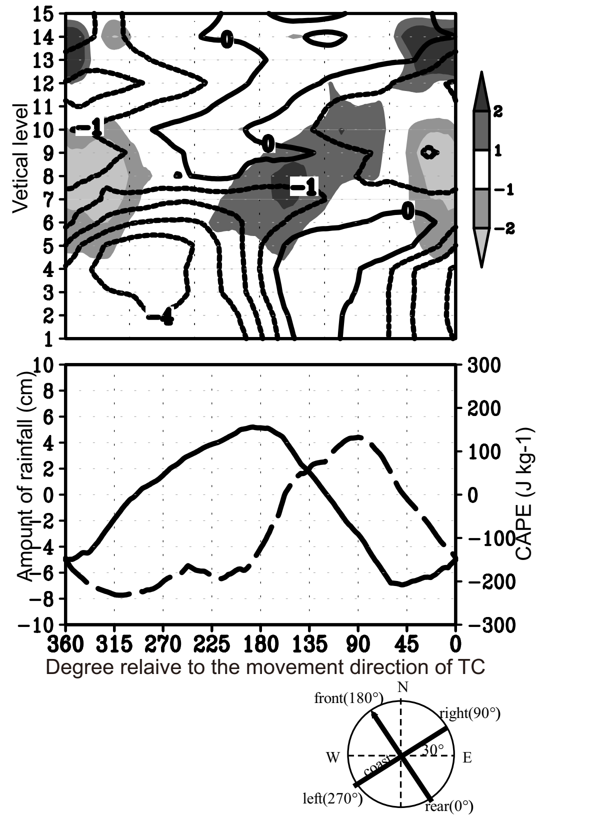

Fig. 8. Anomalies in θ_{se}, vertical motion, CAPE, and rainfall within 100 km of the TC center at each azimuth (average from 11–23 hours; contours: θ_{se}; shading: vertical motion; dashed line: CAPE; solid line: rainfall).

was positive in this area. The downstream advection of this positive instability energy stimulated positive vertical motion. As noted above, CAPE was consistent with θ_{se} at intermediate levels, and the related anomaly in vertical motion occurred mainly at this level, being strongly associated with rainfall. Eventually, the peak in positive rainfall occurred at around 180°, at the front of the TC.

After landfall, drier air made up the entire column of the TC (Fig. 9), although the air at around 90° was wetter than in other quadrants. Consequently, there remained a small positive CAPE anomaly and hence positive vertical motion; rainfall occurred downstream of the TC. Other quadrants of the TC were marked by a negative rainfall anomaly, especially at around 45°, where the rainfall maximum occurred in the control experiment. The negative rainfall anomaly was consistent with a large negative θ_{se} anomaly and enhanced stability of the air.

5. Effect of increased friction

Increased surface roughness affects the precipitation associated with a TC because it increases the inflow of the TC (thereby enhancing the convergence of moisture) and decreases the kinetic energy in the boundary layer; consequently, the decreased wind results in reduced evaporation from the land surface (Tuleya and Kurihara, 1978). CL03 suggested that convergence along the coastline is relatively unimportant in producing rainfall anomalies in the inner area of a TC. In experiment 2 of the present study, increased friction led to enhanced precipitation over a wide area, without affecting the asymmetric structure of the TC. After landfall, the rainfall maximum occurred at the right-front side of the TC, suggesting that the effect of increasing friction over land plays an important role in determining the rainfall distribution of a TC.

The distribution of CAPE in experiment 2 was similar to that in experiment 1, with positive CAPE located mainly from 45°–35° (Fig. 10). The distribution of positive CAPE in experiment 2 relative to the control experiment covered a larger area than in experiment 1, whereas the area of negative CAPE was smaller, meaning that the asymmetrical structure of CAPE was less pronounced. These findings were consistent with the pattern of rainfall in experiment 1. The change in CAPE distribution was probably caused by the suppression of evaporation, as the wind weakened over land. After landfall, the rainfall in experiment 2 showed a marked increase, but a similar CAPE pattern was not observed in this experiment.

Wong and Chan (2006) referred to boundary layer convergence as an indicator of asymmetry forced by the surface when friction is increased. The authors found that the pattern of convergence is consistent with the observed asymmetry in rainfall and vertical motion. In experiment 2 of this study, the temporal evolution of low-level divergence (mean value from σ-level 2–4) showed a consistent pattern with precipitation (Fig. 11). When the TC approached the coastline, the positive convergence became more pronounced on the onshore side of the TC. After landfall, the area of enhanced convergence showed a marked expansion.

As mentioned in section 3.2, after landfall in the present study, the area of most strongly enhanced rainfall shifted from left-front to right-front of the TC, in contrast to the corresponding experiments in CL03. This discrepancy may be related to differences between the studies in terms of the intensity of the vortex due to the beta-effect. After landfall, the MSLP of the vortex in experiments 1 and 2 was about 975 hPa, much higher than that in CL03 (940–950 hPa). Before landfall in experiment 1, the average CAPE peak was located at 90° and the rainfall peak at 90° ahead of CAPE (Fig. 8). After landfall, the CAPE peak remained at around 90°, while the rainfall peak was located at 135° (Fig. 9). This finding indicates that a weaker vortex may act to reduce the distance between

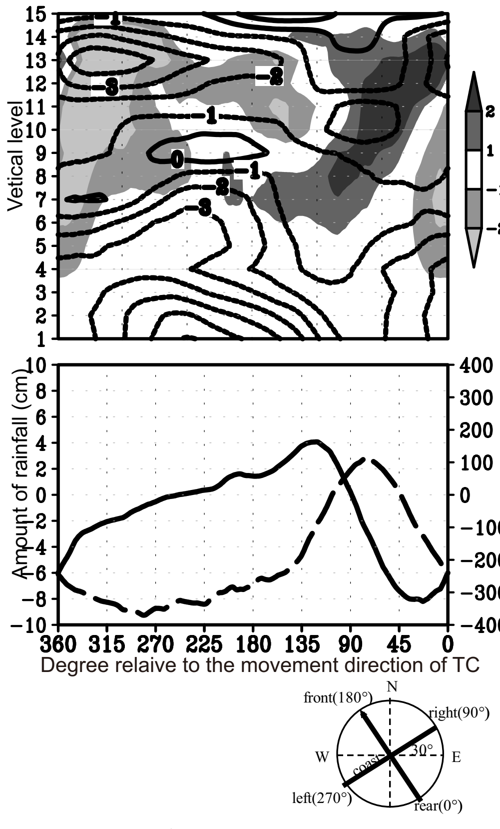

Fig. 9. As Fig. 8, but from 24–36 h.

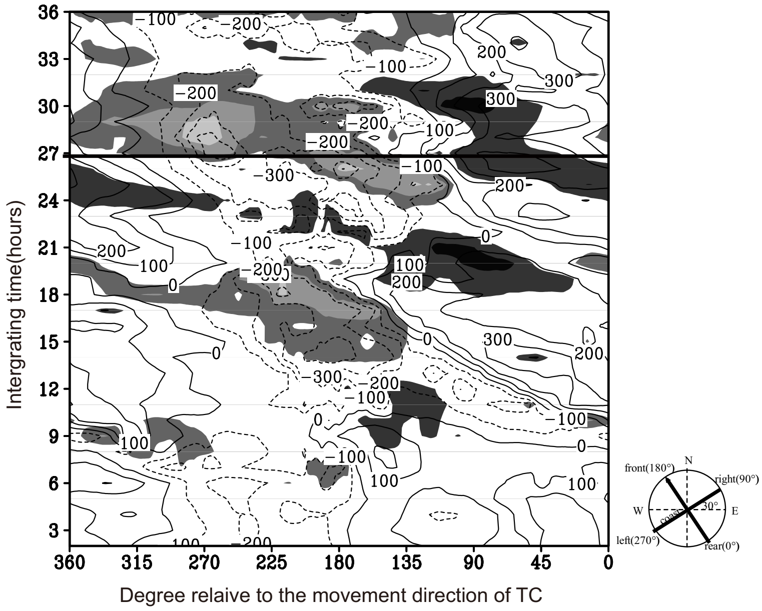

Fig. 10. As Fig. 7, but for experiment 2.

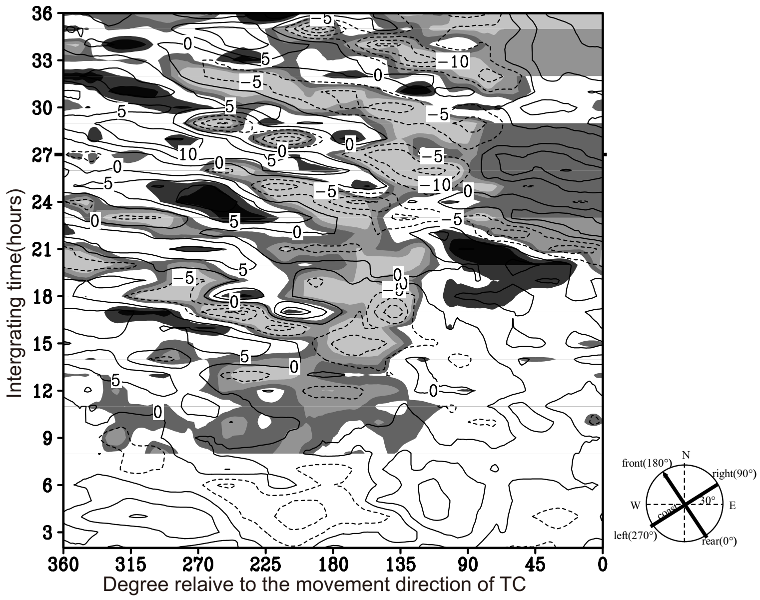

Fig. 11. As Fig. 10, but for low-level divergence (σ-levels 2–4; units: 10^{-5} s^{-1}).

the area of higher CAPE and the enhanced rainfall area, due to weaker advection. In Tuleya and Kurihara (1978), after landfall, the MSLP of the vortex was found to be about 980 hPa in the basic experiment and the location of the maximum precipitation was biased toward the forward-right quadrant, consistent with our assumption that the intensity of the vortex may shift the location of maximum rainfall slightly.

6. Landfall transition process

CL03 studied the convective asymmetries associated with tropical cyclone landfall on an f-plane, revealing that even considering the crude assumptions involved in employing an f-plane, including a moving coastline, as the TC makes landfall the associated convection is modified by changes in surface fluxes over land. The most important factors in this regard are a reduction in moisture flux, which occurs not only via a decrease in moisture supply from the surface, but also via a decrease in wind speed due to increased surface roughness. The changes in rainfall distribution result from the three-dimensional advection of dry air around

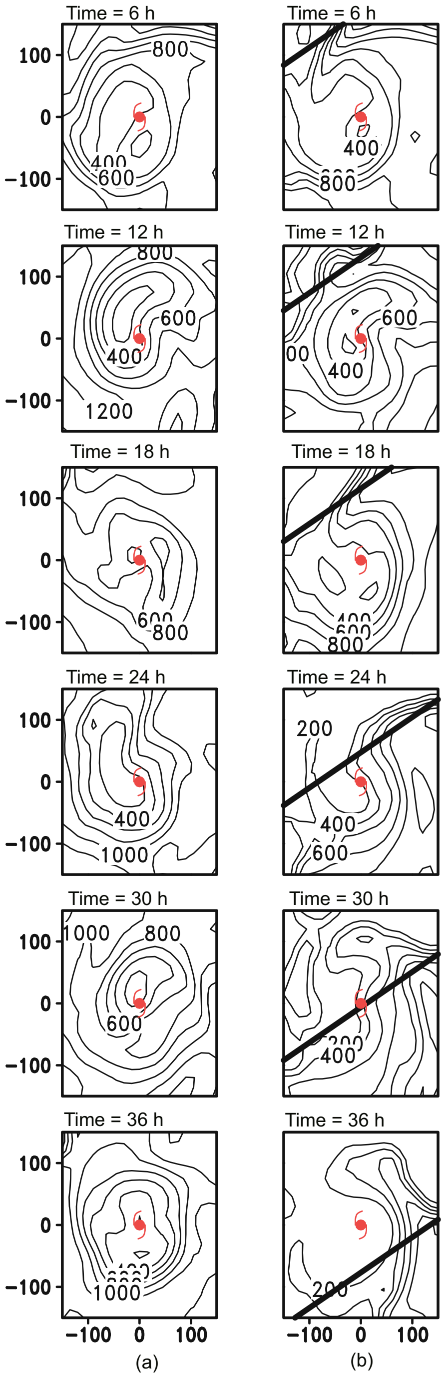

Fig. 12. Distributions of the CAPE index in (a) the control experiment and (b) experiment 1 at 6, 12, 18, 24, 30, and 36 hours. The abscissa and ordinate are the zonal and meridional distance (km) relative to the TC center, which is represented by the typhoon symbol. The thick line indicates the coastline.

the TC, which in turn alters the moist static stability of the atmosphere. Areas in which dry air occurs over moist air are likely to have enhanced convection; consequently, the rainfall maximum occurs at these locations and downstream areas.

The results of the present study revealed that even if the beta-effect was taken into account and the TC moved by itself to make landfall, the most important effect remained a reduction in moisture flux. The dry air from over land and wet air from the sea acted to change the distribution of instability around the TC center, as seen in the distribution of CAPE. Subsequently, positive CAPE upstream of the TC resulted in positive precipitation in downstream areas. Because the extra-tropical transition process (DiMego and Bosart, 1982) is related to baroclinic instability, related in turn to the distribution of cold and warm air, the instability related to dry and wet air during TC landfall was defined here as the landfall transition process. The contrast in instability caused by wet and dry air was defined by CAPE (Fig. 12).

When the cyclone was over the sea, the areas surrounding the TC eye had high values of CAPE, whereas inner areas had low values (Fig. 12a), due to the homogeneous nature of the underlying surface. Once the TC moved toward land, the underlying surface changed, and dry air from the land and wet air from the sea surface were advected into the TC flow. The contrasting properties of the dry and wet air were expected to change the distribution of instability structure, which was represented by CAPE in this study (Fig. 12b). The change in instability (CAPE) led to thermodynamic asymmetry and consequently precipitation asymmetry (data not shown). This process is expected to occur in most TCs upon landfall because of the contrast in latent heat flux between the land and sea surface.

Once a TC makes landfall, in addition to the effects of increased friction and suppressed moisture supply, it is important to consider the effect of the orientation of the coastline. For simplicity, the coastline in the present study was oriented approximately normal to the movement of the TC. Enhanced precipitation occurred mainly on the onshore side of the TC, where the moist air moved from the ocean and air convergence was increased due to increased friction. In fact, when the coastline was rotated cyclonically or anticyclonically, the area of enhanced rainfall rotated accordingly (data not shown). This finding verifies that relatively wet air and convergence along the coastline are the main factors that determine the distribution of precipitation once a TC makes landfall.

7. Summary and discussion

Based on simulations performed using MM5 version 3, this study investigated the convective structure of a TC during landfall and relevant physical processes. A TC-like vortex was placed in a 301 × 301 grid field on a beta-plane. Three experiments were carried out with the following modifications over land: moisture flux turned off, increased surface friction, and these two processes combined. A control experiment was also performed in which these modifications were not made. The coastline was oriented from (0, 95) to (301, 267), thereby ensuring that the TC in the three experiments made landfall at around 27 hours.

On the ß-plane, the maximum rainfall was located from southeast to northeast in the control experiment. When cutting off the moisture supply over land, the rainfall maximum shifted to the right-front quadrant of the TC. Compared with rainfall in the control experiment, positive rainfall was located mainly in the front quadrant of the TC, and rotated anti-cyclonically, similar to that in CL03. When the roughness length was increased over land, the rainfall distribution showed little change before landfall. After landfall, the rainfall maximum moved to the right-front quadrant of the TC. Compared with the control experiment, before landfall, positive rainfall was located in the left-front quadrant of the TC. After landfall, positive rainfall was located in the entire front quadrant of the TC. The cutting off of moisture supply over land suppressed convection in the air mass, while increased friction resulted in increased precipitation in the TC, especially after landfall. When these two factors were combined, the total rainfall in the TC was similar to that in the control experiment.

The cutting off of moisture flux altered the moisture structure of the TC. The drier air occupied a large area at low and intermediate levels in the TC; at the same time, a wetter area occurred in the 80°–45° quadrant of the TC. At high levels, this quadrant was drier than that in the control experiment. The vertical structure of moisture altered the distribution of instability. Subsequently, positive CAPE upstream of the TC caused positive precipitation in downstream areas. The difference between the present results and those in CL03 was high instability resulting from the combination of drier air at high levels and related wetter air at low and intermediate levels.

The distribution of precipitation in experiment 2 was consistent with the distribution of CAPE before landfall. This finding suggests that the main factor determining rainfall distribution may be the suppression of evaporation via reduced wind strength. After landfall, precipitation in experiment 2 was stronger than in experiment 1, whereas CAPE was similar between the two experiments. A strong negative divergence occurred throughout the front quadrant of the TC, consistent with the distribution of precipitation. This implies that increasing convergence caused by the increasing friction may have been another factor in this experiment, especially after landfall.

When a TC makes landfall, in addition to the effect of increasing friction, the suppression of moisture supply and the locations of mountains, it is important to consider the effect of the orientation of the coastline on the distribution of convection. For simplicity, the coastline in the present study was oriented approximately normal to the movement direction of the TC. Enhanced precipitation occurred mainly over land where moist air blew from the ocean and air convergence was enhanced due to increased friction. In fact, when the coastline was rotated cyclonically or anti-cyclonically in the present study, the area of enhanced rainfall rotated accordingly (data not shown). This finding confirms that wet air and convergence along the coastline are the main factors determining the distribution of precipitation once a TC makes landfall.

Acknowledgements. This research was jointly supported by the National Basic Research Program of China (Grant No. 2009CB421500) and the National Natural Science Foundation of China (Grant Nos. 90815028, 40405012 and 40705024).

REFERENCES

Betts, A. K., and M. J. Miller, 1993: The Betts–Miller scheme. *The Representation of Cumulus Convection in Numerical Models, Meteor. Monogr.*, No. 46, Amer. Meteor. Soc., 107–121.

Blackadar, A. K., 1979: High resolution models of the planetary boundary layer. Vol. 1, No. 1, *Advances in Environmental Science and Engineering*, J. Pfaffilin and E. Ziegler, Eds., Gordon and Breach, 50–85.

Blackwell, G. K., 2000: The evolution of Hurricane Danny (1997) at landfall: Doppler-observed eyewall replacement, vortex contraction/ intensification, and low-level wind maxima. *Mon. Wea. Rev.,* **128,** 4002–4016.

Bolton, D., 1980: The computation of equivalent potential temperature. *Mon. Wea. Rev.,* **108**, 1046–1053.

Chan, J. C. L., and R. T. Williams, 1987: Analytical and numerical studies of the beta-effect in tropical cyclone motion. Part I: Zero mean flow. *J. Atmos. Sci.,* **44**(9), 1257–1265.

Chan, J. C. L., and X. Liang, 2003: Convective asymmetries associated with tropical cyclone landfall. part I: f-plane simulations. *J. Atmos. Sci.,* **60,** 1560–1567.

Chan, J. C. L., Y. Duan, and L. K. Shay, 2001: Tropical cyclone intensity change from a simple ocean–atmosphere coupled model. *J. Atmos. Sci.,* **58,** 154–172.

Chan, J. C. L., K. S. Liu, S. E. Ching, and E. S. T. Lai, 2004: Asymmetric distribution of convection associated with tropical cyclones making landfall along the south china coast. *Mon. Wea. Rev.,* **132,** 2411–2420.

Chen, Y., and M. K. Yau, 2003: Asymmetric structures in a simulated landfalling hurricane. *J. Atmos. Sci.,* **60,** 2294–2312.

DiMego, G., and L. F. Bosart, 1982: The transformation of Tropical Storm Agnes into an extratropical cyclone. Part I: The observed fields and vertical motion computations. *Mon. Wea. Rev.*, **110**, 385–411.

Doswell, C. A. III, and E. N. Rasmussen, 1994: The effect of neglecting the virtual temperature correction on CAPE calculations. *Wea. Forecasting*, **9**, 619–623.

Dudhia, J., 1989: Numerical study of convection observed during the Winter Monsoon Experiment using a mesoscale two-dimensional model. *J. Atmos. Sci.,* **46,** 3077–3107.

Dudhia, J., 1993: A nonhydrostatic version of the Penn State/NCAR Mesoscale Model: Validation tests and the simulation of an Atlantic cyclone and cold front. *Mon. Wea. Rev.,* **121,** 1493–1513.

Grell, G., J. Dudahia, and D. R. Stauffer, 1994: A description of the fifth-generation Penn State/NCAR Mesoscale Model (MM5). NCAR Tech. Note NCAR/TN-398 1 STR, 122pp.

Janjic, Z. I., 1994: The step-mountain eta coordinate model: Further developments of the convection, viscous sublayer, and turbulence closure schemes. *Mon. Wea. Rev.,* **122,** 927–945.

Kwok, J. H. Y., and J. C. L. Chan, 2005: The influence of uniform flow on tropical cyclone intensity change. *J. Atmos. Sci.,* **62,** 3193–3212.

Miller, B. I., 1964: A study of the filling of Hurricane Donna (1960) over land. *Mon. Wea. Rev.*, **92**(9), 389–406.

Peng, M. S., B.-F. Jeng, and R. T. Williams, 1999: A numerical study on tropical cyclone intensification. Part I: Beta effect and meanflow effect. *J. Atmos. Sci.,* **56,** 1404–1423.

Powell, M. D., 1982: The transition of the Hurricane Frederic boundary- layer wind field from the open Gulf of Mexico to landfall. *Mon. Wea. Rev.,* **110**(12), 1912–1932.

Powell, M. D., 1987: Changes in the low-level kinematic and thermodynamic structure of Hurricane Alicia (1983) at landfall. *Mon. Wea. Rev.,* **115,** 75–79.

Powell, M. D., and S. H. Houston, 1996: Hurricane Andrew's landfall in south Florida. Part II: Surface wind fields and potential real-time applications. *Wea. Forecasting,* **11,** 329–349.

Powell, M. D., and S. H. Houston, 1998: Surface wind fields of 1995 Hurricanes Erin, Opal, Luis, Marilyn, and Roxanne at landfall. *Mon. Wea. Rev.,* **126,** 1259–1273.

Schneider, R., and G. Barnes, 2005: Low level kinematic, thermodynamic and reflectivity fields associated with hurricane Bonnie (1998) at landfall. *Mon. Wea. Rev.*, **133**, 3243–3259.

Shapiro, L. J., 1983: The asymmetric boundary layer flow under atranslating hurricane. *J. Atmos. Sci.,* **40,** 1984–1998.

Tuleya, R. E., and Y. Kurihara, 1978: A numerical simulation of the landfall of tropical cyclones. *J. Atmos. Sci.,* **35,** 242–257.

Tuleya, R. E., M. A. Bender, and Y. Kurihara, 1984: A simulation study of the landfall of tropical cyclones using a movable nested-mesh model. *Mon. Wea. Rev.,* **112,** 124–136.

Wong, M. L. M., and J. C. L. Chan, 2006: tropical cyclone motion in response to land surface friction. *J. Atmos. Sci.,* **63** 1324–1337.

Zhang, D.-L., and R. A. Anthes, 1982: A high-resolution model of the planetary boundary layer—Sensitivity tests and comparisons with SESAME-79 data. *J. Appl. Meteor.*, **21**, 1594–1609.